Amphiphilic Surface Active Triblock Copolymers with Mixed Hydrophobic and Hydrophilic Side Chains for Tuned Marine Fouling-Release Properties

ARTICLE *in* LANGMUIR · APRIL 2010

Impact Factor: 4.46 · DOI: 10.1021/la100032n · Source: PubMed

Langmuir
Article
pubs.acs.org/Langmuir

Amphiphilic Surface Active Triblock Copolymers with Mixed Hydrophobic and Hydrophilic Side Chains for Tuned Marine Fouling-Release Properties

Daewon Park,[†,#] Craig J. Weinman,[†,#] John A. Finlay,[‡] Benjamin R. Fletcher,[‡] Marvin Y. Paik,[†] Harihara S. Sundaram,[†] Michael D. Dimitriou,[§] Karen E. Sohn,[§] Maureen E. Callow,[‡] James A. Callow,[‡] Dale L. Handlin,[∥] Carl L. Willis,[∥] Daniel A. Fischer,[⊥] Edward J. Kramer,[§] and Christopher K. Ober*[,†]

[†]*Department of Materials Science & Engineering, Cornell University, Bard Hall, Ithaca, New York 14853,* [‡]*School of Biosciences, The University of Birmingham, Birmingham, B15 2TT, U.K.,* [§]*Department of Materials, University of California at Santa Barbara, Santa Barbara, California 93106,* [∥]*KRATON Polymers, Houston, Texas 77082, and* [⊥]*National Institute of Standards and Technology, Gaithersburg, Maryland 20899.*
[#] *These authors contributed equally*

Received January 4, 2010. Revised Manuscript Received March 16, 2010

Two series of amphiphilic triblock surface active block copolymers (SABCs) were prepared through chemical modification of two polystyrene-*block*-poly(ethylene-*ran*-butylene)-*block*-polyisoprene ABC triblock copolymer precursors. The methyl ether of poly(ethylene glycol) [$M_n \approx 550$ g/mol (PEG550)] and a semifluorinated alcohol ($CF_3(CF_2)_9(CH_2)_{10}OH$) [F10H10] were attached at different molar ratios to impart both hydrophobic and hydrophilic groups to the isoprene segment. Coatings on glass slides consisting of a thin layer of the amphiphilic SABC deposited on a thicker layer of an ABA polystyrene-*block*-poly(ethylene-*ran*-butylene)-*block*-polystyrene thermoplastic elastomer were prepared for biofouling assays with algae. Dynamic water contact angle analysis, X-ray photoelectron spectroscopy (XPS) and near-edge X-ray absorption fine structure (NEXAFS) measurements were utilized to characterize the surfaces. Clear differences in surface structure were realized as the composition of attached side chains was varied. In biofouling assays, the settlement (attachment) of zoospores of the green alga *Ulva* was higher for surfaces incorporating a large proportion of the hydrophobic F10H10 side chains, while surfaces with a large proportion of the PEG550 side chains inhibited settlement. The trend in attachment strength of sporelings (young plants) of *Ulva* did not show such an obvious pattern. However, amphiphilic SABCs incorporating a mixture of PEG550 and F10H10 side chains performed the best. The number of cells of the diatom *Navicula* attached after exposure to flow decreased as the content of PEG550 to F10H10 side chains increased.

Introduction

The undesirable consequences of biofouling on ship hulls are well-known[1] and the use of efficient antifouling technology is a necessity. However, antifouling paints that release biocides into the sea are now subject to increasingly stringent regulation and more environmentally benign methods to control fouling are required.[2] The incorporation of tethered, i.e., nonleaching, biocidal moieties into coatings to produce more environmentally friendly antifouling coatings is being actively researched,[3−6] but their use in marine applications has been limited and, thus far, mixed results have been reported.[7−11] Various strategies to control fouling without the use of biocides have been proposed.

The primary mode of attachment of marine organisms to a surface involves the secretion of adhesives, which frequently contain large proportions of proteins and/or glycoproteins.[12−15] Therefore, one approach to controlling fouling is to design minimally adhesive coatings capable of both preventing the attachment of the settling stages of marine organisms and/or promoting low adhesion so that the cells/organisms are easily removed by hydrodynamic forces. The most studied approach to marine biofouling control is to utilize hydrophobic coatings based on poly(dimethylsiloxane) (PDMS) as fouling-release coatings. The low surface energy reduces the polar and hydrogen bonding interactions with the organism's adhesive, effectively lowering adhesive strength, causing macrofouling organisms to be

*To whom correspondence should be addressed. E-mail: cko3@cornell.edu. Telephone: 607-255-8417. Fax: 607-255-2365.

(1) Schultz, M. P. *Biofouling* **2007**, *23*, 331−341.
(2) Krishnan, S.; Weinman, C. J.; Ober, C. K. *J. Mater. Chem.* **2008**, *18*, 3405−3413.
(3) Sauvet, G.; Dupond, S.; Kazmierski, K.; Chojnowski, J. *J. Appl. Polym. Sci.* **2000**, *75*, 1005−1012.
(4) Krishnan, S.; Ward, R. J.; Hexemer, A.; Sohn, K. E.; Lee, K. L.; Angert, E. R.; Fischer, D. A.; Kramer, E. J.; Ober, C. K. *Langmuir* **2006**, *22*, 11255−11266.
(5) Park, D.; Wang, J.; Klibanov, A. M. *Biotechnol. Prog.* **2006**, *22*, 584−589.
(6) Kurt, P.; Wood, L.; Ohman, D. E.; Wynne, K. J. *Langmuir* **2007**, *23*, 4719−4723.
(7) Park, D.; Finlay, J. A.; Ward, R. J.; Weinman, C. J.; Krishnan, S.; Paik, M. Y.; Sohn, K. E.; Callow, M. E.; Callow, J. A.; Handlin, D. L.; Willis, C. L.; Fischer, D. A.; Angert, E. R.; Kramer, E. J.; Ober, C. K. *ACS Appl. Mater. Interfaces* **2010**, Articles ASAP.
(8) Majumdar, P.; Lee, E.; Patel, N.; Stafslien, S. J.; Daniels, J.; Chisholm, B. J. *J. Coat. Technol. Res.* **2008**, *5*, 405−417.
(9) Majumdar, P.; Lee, E.; Patel, N.; Ward, K.; Stafslien, S. J.; Daniels, J.; Chisholm, B. J.; Boudjouk, P.; Callow, M. E.; Callow, J. A.; Thompson, S. E. M. *Biofouling* **2008**, *24* (3), 185−200.
(10) Krishnan, S.; Finlay, J. A.; Hexemer, A.; Wang, N.; Ober, C. K.; Kramer, E. J.; Callow, M. E.; Callow, J. A.; Fischer, D. A. *Polym. Prepr.* (*Am. Chem. Soc., Div. Polym. Chem*) **2005**, *46*, 1248−1249.
(11) Ye, S.; McClelland, A.; Majumdar, P.; Stafslien, S. J.; Daniels, J.; Chisholm, B.; Chen, Z. *Langmuir* **2008**, *24*, 9686−9694.
(12) Finlay, J. A.; Callow, M. E.; Ista, L. K.; Lopez, G. P.; Callow, J. A. *Integr. Comp. Biol.* **2002**, *42*, 1116−1122.
(13) Yamamoto, H.; Sakai, Y.; Ohkawa, K. *Biomacromolecules* **2000**, *1*, 543−551.
(14) Smith, A. M.; Callow, J. A. *Biological Adhesives*. Springer: Berlin, 2006.
(15) Aldred, N. A.; Clare, A. S. *Biofouling* **2008**, *24*, 351−363.
(16) Brady, R. F.; Singer, I. L. *Biofouling* **2000**, *15*, (1−3), 73−81.
(17) Kavanagh, C. J.; Quinn, R. D.; Swain, G. W. *J. Adhes.* **2005**, *81*, 843−868.
(18) Wendt, D. E.; Kowalke, G. L.; Kim, J.; Singer, I. L. *Biofouling* **2006**, *22*, 1−9.

"released" from the soft elastomeric coating by applied shear.[16−20] Many recent studies have been aimed at improving the mechanical properties[18,21−25] or fabricating topographic features in PDMS aimed at reducing the settlement of spores and larvae.[26,27] Fluorosiloxanes[28,29] and fluoropolymers[30−32] have also been investigated as fouling-release coatings.

An alternative approach to low energy elastomeric coatings is the fabrication of protein repellant surfaces incorporating poly(ethylene glycol) (PEG) based (co)polymers. PEG, an uncharged, water-soluble polymer has inherent antifouling efficacy since it is hydrophilic and its long, flexible chains contribute to its ability to uniquely coordinate with surrounding water molecules. It is believed that the superior ability of PEG to be hydrated with water molecules, in conjunction with steric exclusion effects, are both crucial to resisting the adsorption of proteins.[33−35] Many protein-resistant materials incorporating PEG have been reported in the literature, ranging from the combination with poly(methyl methacrylate) as a potential material for biomedical devices,[36] to PEG containing self-assembled monolayers[37,38] and polymer brushes[39] to form protein resistant functional coatings. In the area of marine antifouling, PEG monolayers[40−44] and PEGylated hydrogels,[45] as well as multilayer coatings based on surface active block copolymers with grafted PEG side chains,[46,47] have all been evaluated for their resistance to the settlement (attachment) of certain fouling organisms.

Recently, several amphiphilic fouling release coatings have been reported that combine hydrophobic, low surface energy fluorinated moieties with protein resistant hydrophilic PEG containing groups. Gudipati et al. reported the development of coatings consisting of an amphiphilic network of hyperbranched fluoropolymer groups combined with linear PEG moieties that showed better release of sporelings of the green seaweed *Ulva* than a PDMS coating.[48] Additionally, in two separate studies, Krishnan et al.[49] and Martinelli et al.[50] reported side-chain block copolymers containing grafted ethoxylated fluoroalkyl groups that were capable of releasing both sporelings (young plants) of *Ulva* and diatoms (unicellular algae). The results suggested that amphiphilic coatings have the potential to resist both the attachment and adhesion of algae which employ different strategies for settlement and adhesion.

A potential shortcoming of these prior approaches is the use of nonionic surfactant moieties as the basis of the amphiphilic structure. By covalently linking the polar and nonpolar groups as a single unit the molecular mixing of the two components is assured; however, the ability to alter their relative composition is limited in the polymer modification stage because each group must be specifically prepared. Instead by introducing these groups separately, it may be possible to achieve the same amphiphilic behavior with the added benefit that the relative composition and therefore the surface properties can be easily tuned.

The following study reports the development of amphiphilic polymeric coatings that combine low surface energy with resistance to cell adhesion through the random incorporation of discrete poly(ethylene glycol) and semifluorinated side chains with two polystyrene-*block*-poly(ethylene-*ran*-butylene)-*block*-polyisoprene, PS-*b*-P(E/B)-*b*-PI, ABC triblock copolymer precursors. The molecular size of the polystyrene and the poly(ethylene-*ran*-butylene) blocks of these triblock copolymers were tailored to match those of the polystyrene-*block*-poly(ethylene-*ran*-butylene)-*block*-polystyrene thermoplastic elastomer. In addition, we have varied the length of the terminal polyisoprene block to establish how the surface active segment length influences surface activity.

Chemical characterization of the resultant surface active block copolymers (SABCs) are reported below and correlated to surface characterization using near-edge X-ray adsorption fine structure (NEXAFS) analysis, X-ray photoelectron spectroscopy (XPS) and dynamic water contact angle analysis. Additionally, biofouling assays carried out on a set of amphiphilic SABCs indicate the ability of these materials to resist and release fouling by both the green macroalga *Ulva* and the diatom *Navicula*. *Ulva* (formerly *Enteromorpha*) is the most common macroalga ("seaweed") contributing to "soft" fouling of man-made surfaces throughout the world. Fouling is initiated by the settlement (attachment) and subsequent adhesion of motile, quadriflagellate zoospores

(19) Kim, J.; Chisholm, B. J.; Bahr, J. *Biofouling* **2007**, *23*, 113−120.
(20) Kim, J.; Nyren-Erikson, E.; Stafslien, S.; Daniels, J.; Bahr, J.; Chisholm, B. J. *Biofouling* **2008**, *24*, 313−319.
(21) Brady, R. F. *J. Protect. Coat. Linings* **2003**, *20* (1), 33−37.
(22) Beigbeder, A.; Degee, P.; Conlan, S. L.; Mutton, R. J.; Clare, A. S.; Pettitt, M. E.; Callow, M. E.; Callow, J. A.; Dubois, P. *Biofouling* **2008**, *24*, 291−302.
(23) Pieper, R. J.; Ekin, A.; Webster, D. C.; Casse, F.; Callow, J. A.; Callow, M. E. *J. Coat. Technol. Res.* **2007**, *4* (4).
(24) Ekin, A.; Webster, D. C.; Daniels, J. W.; Stafslien, S. J.; Casse, F.; Callow, J. A.; Callow, M. E. *J. Coat. Technol. Res.* **2007**, *4*, 435−451.
(25) Callow, M. E.; Callow, J. A. *Biofouling* **2000**, *13*, 157−172.
(26) Schumacher, J. F.; Aldred, N.; Callow, M. E.; Finlay, J. A.; Callow, J. A.; Clare, A. S.; Brennan, A. B. *Biofouling* **2007**, *23*, 307−317.
(27) Schumacher, J. F.; Carman, M. L.; Estes, T. G.; Feinberg, A. W.; Wilson, L. H.; Callow, M. E.; Callow, J. A.; Finlay, J. A.; Brennan, A. B. *Biofouling* **2007**, *23*, 55−62.
(28) Grunlan, M. A.; Lee, N. S.; Cai, G.; Gaedda, T.; Mabry, J. M.; Mansfield, F.; Kus, E.; Wendt, D. E.; Kowalke, G. L.; Finlay, J. A.; Callow, J. A.; Callow, M. E.; Weber, W. P. *Chem. Mater.* **2004**, *16*, 2433−2441.
(29) Marabotti, I.; Morelli, A.; Orsini, L. M.; Martinelli, E.; Galli, G.; Chiellini, E.; Lien, E. M.; Pettitt, M. E.; Callow, J. A.; Conlan, S. L.; Mutton, R. J.; Clare, A. S.; Kocijan, A.; Donik, C.; Jenko, M. *Biofouling* **2009**, *25*, 481−493.
(30) Yarbrough, J. C.; Rolland, J. P.; DeSimone, J. M.; Callow, M. E.; Finlay, J. A.; Callow, J. A. *Macromolecules* **2006**, *39*, 2521−2528.
(31) Hu, Z.; Chen, L.; Betts, D.; Pandya, A.; Hillmyer, M. A.; DeSimone, J. M. *J. Am. Chem. Soc.* **2008**, *130*, 14244−14252.
(32) Hu, Z.; Finlay, J. A.; Chen, L.; Betts, D. E.; Hillmyer, M. A.; Callow, M. E.; Callow, J. A.; DeSimone, J. M. *Macromolecules* **2009**, *42*, (18), 6999−7007.
(33) Unsworth, L. D.; Sheardown, H.; Brash, J. L. *Langmuir* **2005**, *21*, (3), 1036−1041.
(34) Li, L.; Chen, S.; Zheng, J.; Ratner, B. D.; Jiang, S. *J. Phys. Chem. B* **2005**, *109*, 2934−2941.
(35) Luk, Y.-Y.; Kato, M.; Mrksich, M. *Langmuir* **2000**, *16*, 9604−9608.
(36) Walton, D. G.; Soo, P. P.; Mayes, A. M.; Allgor, S. J. S.; Fujii, J. T.; Griffith, L. G.; Ankner, J. F.; Kaiser, H.; Johansson, J.; Smith, G. D. *Macromolecules* **1997**, *30*, 6947−6956.
(37) Mrksich, M.; Whitesides, G. M. *ACS Symp. Ser.* **1997**, *680*, 361−373.
(38) Prime, K. L.; Whitesides, G. M. *J. Am. Chem. Soc.* **1993**, *115*, 10714−10721.
(39) Ma, H.; Hyun, J.; Stiller, P.; Chilkoti, A. *Adv. Mater.* **2004**, *16*, 338−341.
(40) Callow, M. E.; Callow, J. A.; Ista, L. K.; Coleman, S. E.; Nolasco, A. C.; Lopez, G. P. *Appl. Environ. Microbiol.* **2000**, *66*, 3249−3254.
(41) Finlay, J. A.; Krishnan, S.; Callow, M. E.; Callow, J. A.; Dong, R.; Asgill, N.; Wong, K.; Kramer, E. J.; Ober, C. K. *Langmuir* **2008**, *24*, 503−510.
(42) Schilp, S.; Kueller, A.; Rosenhahn, A.; Grunze, M.; Pettitt, M. E.; Callow, M. E.; Callow, J. A. *Biointerphases* **2007**, *2*, 143−150.
(43) Statz, A.; Finlay, J. A.; Dalsin, J.; Callow, M. E.; Callow, J. A.; Messersmith, P. B. *Biofouling* **2006**, *22*, 391−399.
(44) Schilp, S.; Rosenhahn, A.; Pettiitt, M. E.; Bowen, J.; Callow, M. E.; Callow, J. A.; Grunze, M. *Langmuir* **2009**, *25*, 10077−10082.
(45) Ekblad, T.; Bergstrom, G.; Ederth, T.; Conlan, S. L.; Mutton, R.; Clare, A. S.; Wang, S.; Liu, Y.; Zhao, Q.; D'Souza, F.; Donnelly, G. T.; Willemsen, P. R.; Pettitt, M. E.; Callow, M. E.; Callow, J. A.; Liedberg, B. *Biomacromolecules* **2008**, *9*, 2775−2783.
(46) Youngblood, J. P.; Andruzzi, L.; Ober, C. K.; Hexemer, A.; Kramer, E. J.; Callow, J. A.; Finlay, J. A.; Callow, M. E. *Biofouling* **2003**, *19*, 91−98.
(47) Krishnan, S.; Wang, N.; Ober, C. K.; Finlay, J. A.; Callow, M. E.; Callow, J. A.; Hexemer, A.; Sohn, K. E.; Kramer, E. J.; Fischer, D. A. *Biomacromolecules* **2006**, *7*, 1449−1462.
(48) Gudipati, C. S.; Finlay, J. A.; Callow, J. A.; Callow, M. E.; Wooley, K. L. *Langmuir* **2005**, *21*, 3044−3053.
(49) Krishnan, S.; Ayothi, R.; Hexemer, A.; Finlay, J. A.; Sohn, K. E.; Perry, R.; Ober, C. K.; Kramer, E. J.; Callow, M. E.; Callow, J. A.; Fischer, D. A. *Langmuir* **2006**, *22*, 5075−5086.
(50) Martinelli, E.; Agostini, S.; Galli, G.; Chiellini, E.; Glisenti, A.; Pettiitt, M. E.; Callow, M. E.; Callow, J. A.; Graf, K.; Bartels, F. W. *Langmuir* **2008**, *24*, 13138−13147.

Scheme 1. Synthesis of Semifluorinated 10-Perfluorodecyl-1-decanol (F10H10OH)

(approximately 7−8 μm in length), which form the starting point of the assays.[51] The swimming spores settle and adhere through discharge of a glycoprotein adhesive,[52] and then they rapidly germinate into sporelings (young plants). The strength of attachment of sporelings to experimental coatings was evaluated under hydrodynamic shear using a calibrated water jet. The second test alga was the diatom *Navicula*. Diatoms are unicellular algae that form biofilms (slimes) on surfaces.[53] Unlike *Ulva* spores that are motile and therefore able to "select" where to settle, diatom cells are not motile in the water column and reach a surface through transport in currents and gravity. In laboratory assays, the cells sink rapidly and form an even covering on the test surfaces. Any differences in the number of cells attached after gentle washing indicates their ability to adhere to a particular surface. A flow channel was used to measure how strongly the cells adhere to a surface. The reason for using both *Ulva* and *Navicula* to evaluate test coatings is because the differences in their adhesion biology result in different responses to surfaces. For example, sporelings of *Ulva* adhere weakly to low energy coatings such as silicones, but diatoms adhere strongly to this type of coating.[54]

Experimental Section

Materials. Both the polystyrene$_{8K}$-*block*-poly(ethylene-*ran*-butylene)$_{25K}$-*block*-polyisoprene$_{10K}$ (PS_{8K}-*b*-$P(E/B)_{25K}$-*b*-PI_{10K}) and the polystyrene$_{8K}$-*block*-poly(ethylene-*ran*-butylene)$_{25K}$-*block*-polyisoprene$_{20K}$ (PS_{8K}-*b*-$P(E/B)_{25K}$-*b*-PI_{20K}) triblock precursor copolymers were produced using anionic polymerization and subsequent catalytic hydrogenation by Kraton Polymers at pilot plant scale (~0.5 kg). The subscripts represent the number-average molecular weights of the blocks in kg/mol.

1-Iodoperfluorodecane ($I(CF_2)_{10}F$, FW 648.98, 98%) was purchased from Synquest Laboratories and used as received. 9-Decen-1-ol ($H_2C{=}CH(CH_2)_8OH$, FW 156.27, 97%), 2,2′-azobis(isobutyronitrile) (AIBN, $N{\equiv}CC(CH_3)_2N{=}NC(CH_3)_2C{\equiv}N$, FW 164.21, 98%), and tributyltin hydride ($(n\text{-}Bu)_3SnH$, FW 291.06, 97%) were purchased from Sigma-Aldrich and used as received in conjunction with the 1-iodoperfluorodecane to synthesize 10-perfluorodecyl-1-decanol (F10H10OH, $F(CF_2)_{10}(CH_2)_{10}$-OH, FW 676.35).

3-*meta*-Chloroperoxybenzoic acid (*m*CPBA, ClC_6H_4COOOH, FW 172.57, 77%), boron trifluoride diethyl etherate ($BF_3{\cdot}Et_2O$, $BF_3{\cdot}O(CH_2CH_3)_2$, FW 141.93, 99.9%), and poly(ethylene glycol) methyl ether (PEG550, $CH_3(OCH_2CH_2)_xOH$, average $M_n \approx 550$, $x \approx 12$) were also purchased from Sigma-Aldrich and used as received in the modification of the PS-*b*-P(E/B)-*b*-PI triblock precursor polymers. Anhydrous chloroform ($CHCl_3$), anhydrous toluene, and anhydrous α,α,α-trifluorotoluene (TFT) were purchased from Sigma-Aldrich and used with no further purification. Chloroform, dichloromethane (CH_2Cl_2), methanol, toluene, 6.25 N sodium hydroxide, 96% sulfuric acid, 30 wt % hydrogen peroxide in water, 95% ethanol, and all other reagents were used as received.

3-(Glycidoxypropyl)trimethoxysilane (GPS, 99%) was purchased from Gelest and used as received. Two separate polystyrene-*block*-poly(ethylene-*ran*-butylene)-*block*-polystyrene (SEBS) triblock thermoplastic elastomers (Kraton G1652 and Kraton MD6945) and SEBS grafted with maleic anhydride (MA-SEBS, Kraton FG1901X) were generously provided by Kraton Polymers.

Characterization. ^{1}H NMR spectra were recorded using a Varian Gemini spectrometer with deuterated chloroform. The IR spectra of the polymers cast as films from THF solution on sodium chloride plates was collected using a Mattson 2020 Galaxy Series FTIR spectrometer. Elemental analysis for weight percent C, H, and F of the surface active block copolymers was performed by Quantitative Technologies, Inc. (QTI). Gel permeation chromatography of a THF solution of polymers (1 mg/mL) was carried out using four Waters Styragel HT columns operating at 40 °C in conjunction with Waters 490 ultraviolet (λ = 254 nm) and Waters 410 refractive index detectors. The molecular weight range of the columns was from 500 to 10^7 g/mol. THF was used as the eluent at a flow rate of 1 mL/min, and toluene was used as a marker for flow calibration.

Synthesis of 10-Perfluorodecyl-1-decanol (F10H10OH). The semifluorinated alcohol, 10-perfluorodecyl-1-decanol (F10H10OH) was produced in a manner analogous to that reported in Hopken et al.[55] The reaction scheme is given in Scheme 1. 9-Decen-1-ol (14.07 g, 0.09 mol) and perfluorodecyl iodide (38.76 g, 0.06 mol) were taken in a round-bottom flask fitted with a condenser and septa. The reactants were purged with argon and the mixture was heated to 90 °C while stirring. AIBN (300 mg) was added incrementally over a period of 45 min. After 5 h, the reaction temperature was reduced to 80 °C and 30 mL of anhydrous toluene was added, followed by additional AIBN (1.5 g) and tributyl tin hydride (52.38 g, 0.18 mol). The reaction mixture was stirred while heating at 80 °C for 24 h and then an additional 60 mL of anhydrous toluene was added to the reaction mixture, which was then allowed to cool to room temperature. The raw F10H10OH product crystallized out of solution as a white solid and was collected by filtration and subsequently recrystallized from hot toluene three times to remove residual starting products and tributyl tin impurities. Finally, the purified F10H10OH was dried under reduced pressure at room temperature for 48 h.

^{1}H NMR for F10H10OH (300 MHz, $CDCl_3$, δ): 3.63 (q, 2H, $HO\mathbf{CH_2}CH_2-$), 2.07 (m, 2H, $-CH_2\mathbf{CH_2}CF_2-$), 1.58 (m, 2H, $-CF_2CH_2\mathbf{CH_2}CH_2-$); 1.30 (br s, 12H, $-CF_2-CH_2-CH_2-(\mathbf{CH_2})_6-$ and 1H, $-\mathbf{H}OCH_2-$). IR (dry film) υ_{max} (cm $^{-1}$): 3250 (O−H stretching); 2925, 2850 (C−H stretching); 1470, 1452 (C−H bending); 1330−1095 (C−F stretching); 1055 (C−O stretch).

Polymer Synthesis and Characterization. Surface active block copolymers were produced through a straightforward two step modification of the Kraton PS-*b*-P(E/B)-*b*-PI precursor polymers depicted in Scheme 2, in similar fashion to that previously reported by Weinman et al.[56,57] Functionalization of the PI block was achieved through epoxidation of the residual alkene groups followed by subsequent catalytic ring-opening etherification reactions using alcohols carrying functionality.

(51) Callow, M. E.; Callow, J. A.; Pickett-Heaps, J. D.; Wetherbee, R. *J. Phycol.* **1997**, *33*, 938−947.
(52) Callow, J. A.; Callow, M. E. The *Ulva* spore adhesive system. In *Biological Adhesives*, Smith, A. M.; Callow, J. A., Eds.; Springer: Berlin, 2006; pp 63−78.
(53) Molino, P. J.; Wetherbee, R. *Biofouling* **2008**, *24*, 365−379.
(54) Casse, F.; Ribeiro, E.; Ekin, A.; Webster, D. C.; Callow, J. A.; Callow, M. E. *Biofouling* **2007**, *23*, 267−276.
(55) Hopken, J.; Moller, M.; Boileau, S. *New Polym. Mater.* **1991**, *2*, 339−356.
(56) Weinman, C. J.; Finlay, J. A.; Park, D.; Paik, M. Y.; Krishnan, S.; Fletcher, B. R.; Callow, M. E.; Callow, J. A.; Handlin, D. L.; Willis, C. L.; Fischer, D. A.; Sohn, K. E.; Kramer, E. J.; Ober, C. K., Antifouling, A. B. C. *Polym. Mater.: Sci. Eng. Prepr.* **2008**, *98*, 639−640.
(57) Weinman, C. J.; Finlay, J. A.; Park, D.; Paik, M. Y.; Krishnan, S.; Sundaram, H. S.; Dimitriou, M.; Sohn, K. E.; Callow, M. E.; Callow, J. A.; Handlin, D. L.; Willis, C. L.; Kramer, E. J.; Ober, C. K. *Langmuir* **2009**, *25*, 12266−12274.

Scheme 2. Synthesis of Ether-Linked Surface Active Triblock Copolymers Containing PEG550 and/or F10H10 Side Chains[a]

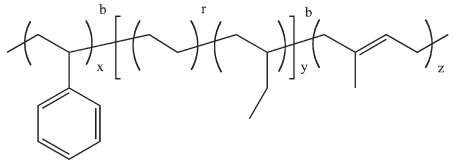

PS-*b*-P(E/B)-*b*-PI Triblock Copolymer

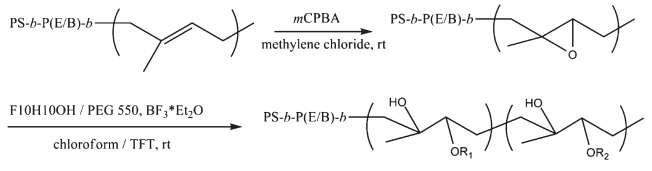

[a] $R_1 = -O(CH_2)_{10}(CF_2)_{10}F$; $R_2 = -(OCH_2CH_2)_{12}OCH_3$.

Two precursor block copolymers were used in our studies, PS_{8K}-*b*-$P(E/B)_{25K}$-*b*-PI_{10K} and PS_{8K}-*b*-$P(E/B)_{25K}$-*b*-PI_{20K}. In a typical epoxidation reaction, the PS_{8K}-*b*-$P(E/B)_{25K}$-*b*-PI_{10K} SABC precursor polymer (5 g, 14.5 mmol of reactive isoprene sites) was dissolved in 100 mL of dichloromethane in a round bottomed flask. 3-Chloroperoxybenzoic acid (*m*CPBA, 3.9 g, 17.4 mmol) was added to the mixture, and the solution was stirred vigorously for 5 h at room temperature. Subsequently, the polymer was precipitated in methanol, collected by filtration, and reprecipitated from dichloromethane to remove residual *m*CPBA and its respective byproducts. The white, rubbery product was dried at room temperature under reduced pressure for 48 h to remove remaining solvent. An analogous reaction and work-up was used to successfully epoxidize the PS_{8K}-*b*-$P(E/B)_{25K}$-*b*-PI_{20K} SABC precursor polymer, scaled to 25 mmol of reactive isoprene sites per 5 g of precursor polymer.

^{1}H NMR for epoxidized PS_{8K}-*b*-$P(E/B)_{25K}$-*b*-PI_{10K} (300 MHz, $CDCl_3$, δ): 6.57, 7.07, (5H, styrene), 2.66 (br s, 1H, epoxidized isoprene, $-CH_2\mathbf{HCOC}(CH_3)CH_2-$), 0.80, 1.07, 1.22, 1.45, 1.57 (backbone). IR (dry film) υ_{max} (cm $^{-1}$): 2925, 2850 (C−H stretching); 1470 (C−H bending); 1070 (C−O stretching); 880 (C−O−C stretching); 700 (C−H bending, aromatic).

^{1}H NMR for epoxidized PS_{8K}-*b*-$P(E/B)_{25K}$-*b*-PI_{20K} (300 MHz, $CDCl_3$, δ): 6.6, 7.1, (5H, styrene), 2.7 (br s, 1H, epoxidized isoprene, $-CH_2\mathbf{HCOC}(CH_3)CH_2-$), 0.8, 1.1, 1.2, 1.45, 1.6 (backbone). IR (dry film) υ_{max} (cm $^{-1}$): 2925, 2850 (C−H stretching); 1470 (C−H bending); 1070 (C−O stretching, weak); 880 (C−O−C stretching, weak); 700 (C−H bending, aromatic, weak).

To produce ether-linked side chain surface active block copolymers, 2.1 g of epoxidized PS_{8K}-*b*-$P(E/B)_{25K}$-*b*-PI_{10K} (5.8 mmol of epoxide), for example, was taken in a round-bottom flask in conjunction with a four times molar excess (23.2 mmol) of side-chain precursor alcohol (F10H10OH and/or PEG550). Seven different mixtures of F10H10OH relative to PEG550 were used in the feed to produce a range of different SABCs: 100% F10H10OH, 80% F10H10OH/20% PEG550, 60% F10H10OH/40% PEG550, 50% F10H10OH/50% PEG550, 40% F10H10OH/60% PEG550, 20% F10H10OH/80% PEG550 and 100% PEG550. The reactants were purged with argon and subsequently dissolved in ca. 150 mL of anhydrous chloroform. Anhydrous TFT was added as necessary to solvate the F10H10OH (indicated by the formation of a clear solution). Activated molecular sieves were added to dry the reaction mixture of any residual moisture. The mixture was allowed to sit for ~12 h, and then was transferred via canula to a fresh reactor to effectively separate the mixture from the sieves. Etherification was performed through the addition of boron trifluoride diethyl etherate catalyst (0.345 g, 2.4 mmol) followed by vigorous stirring at room temperature for at least 48 h. Following the reaction, 6.25 N sodium hydroxide was added to quench any residual boron catalyst and the reaction mixture was concentrated under reduced pressure using a rotary evaporator. The resultant surface active triblock copolymers were precipitated into methanol, with water added as necessary to help isolate the PEGylated samples. The SABCs were collected by filtration and subsequently reprecipitated twice from chloroform to remove additional residual surface active side-chain alcohol precursors. Finally, the finished samples were dried under reduced pressure at room temperature for 48 h to fully remove residual solvent. ^{1}H NMR and IR characterization of representative samples are provided below.

^{1}H NMR for PS_{8K}-*b*-$P(E/B)_{25K}$-*b*-PI_{10K} functionalized with PEG550 side chains (300 MHz, $CDCl_3$, δ): 6.56, 7.08, (5H, styrene), 3.63 (br s, 4H $-O\mathbf{CH_2CH_2}O-$); 3.38 (s, 3H, -$O\mathbf{CH_3}$); 2.24 (s, 1H, -**OH**); 0.83, 1.06, 1.24, 1.80 (backbone). IR (dry film) υ_{max} (cm $^{-1}$): 3350 (O−H stretching); 2935, 2865 (C−H stretching); 1455, 1375 (C−H bending); 1120 (C−O stretching); 700 (C−H bending, aromatic). Anal.: C, 76.1; H, 11.7.

^{1}H NMR for PS_{8K}-*b*-$P(E/B)_{25K}$-*b*-PI_{10K} functionalized with F10H10 side chains (300 MHz, $CDCl_3$, δ): 6.57, 7.07, (5H, styrene), 3.50 (br m, 2H $-O\mathbf{CH_2}CH_2-$); 2.40 (br s, 2H $-CH_2$-$\mathbf{CH_2}CF_2-$); 0.82, 1.04, 1.24, 1.57, 2.03 (backbone, $-OCHH_2$-$(\mathbf{CH_2})_8CH_2CF_2$). IR (dry film) υ_{max} (cm $^{-1}$): 3480 (O−H stretching); 2930, 2860 (C−H stretching); 1460, 1380 (C−H bending); 1220 (C−F stretching); 1090 (C−O stretching); 700 (C−H bending, aromatic). Anal.: C, 67.5; H, 9.4; F, 18.3. Surface-active block copolymers incorporating both types of side chain were found to have a blend of peaks that correlated to the amount of incorporation of each moiety; see below.

^{1}H NMR for PS_{8K}-*b*-$P(E/B)_{25K}$-*b*-PI_{20K} functionalized with PEG550 side chains (300 MHz, $CDCl_3$, δ): 6.6, 7.1, (5H, styrene), 3.6 (br s, 4H $-O\mathbf{CH_2CH_2}O-$); 3.4 (s, 3H, -$O\mathbf{CH_3}$); 2.2 (s, 1H, −**OH**, weak); 0.8, 1.1, 1.24, 1.8 (polymer backbone).

^{1}H NMR for PS_{8K}-*b*-$P(E/B)_{25K}$-*b*-PI_{20K} functionalized with F10H10 side chains (300 MHz, $CDCl_3$, δ): 6.6, 7.1, (5H, styrene), 3.5 (br m, 2H $-O\mathbf{CH_2}CH_2-$); 2.4 (br s, 2H $-CH_2\mathbf{CH_2}CF_2-$); 0.8, 1.0, 1.2, 1.6, 2.0 (polymer backbone, $-OCHH_2(\mathbf{CH_2})_8$-CH_2CF_2-).

^{1}H NMR for PS_{8K}-*b*-$P(E/B)_{25K}$-*b*-PI_{20K} functionalized with both PEG550 (60% by weight feed ratio) and F10H10 side chains (40% by weight feed ratio) (300 MHz, $CDCl_3$, δ): 6.6, 7.1, (5H, styrene), 3.6 (br m, 2H $-O\mathbf{CH_2}-$); 3.4 (s, 3H, $-O\mathbf{CH_3}$); 2.4 (br s, 2H $-CH_2\mathbf{CH_2}CF_2-$); 0.8, 1.0, 1.2, 1.6, 2.0 (polymer backbone, $-OCHH_2(\mathbf{CH_2})_8CH_2CF_2$-). IR (dry film) υ_{max} (cm $^{-1}$): 3480 (O−H stretching); 2930, 2860 (C−H stretching); 1460, 1380 (C−H bending); 1220 (C−F stretching); 1090 (C−O stretching); 700 (C−H bending, aromatic).

Surface Preparation and Characterization. Surfaces for NEXAFS measurements, XPS, and dynamic water contact angle analysis were prepared on silicon wafers by spin-coating 3% (w/v) solutions of SABCs in TFT at 2000 rpm for 60 s. All surfaces prepared for study were annealed in a vacuum oven at reduced pressure at 120 °C for at least 12 h followed by slow cooling to room temperature. Film thickness on Si for these studies was found to be on the order of ca. 100 nm.

XPS measurements were performed using a Kratos Axis Ultra Spectrometer (Kratos Analytical, Manchester, UK) with a monochromatic Al Kα X-ray source (1486.6 eV) operating at 225 W under a vacuum of $1.0 \times 10-8$ Torr. Charge compensation was carried out by injection of low-energy electrons into the magnetic lens of the electron spectrometer. The pass energy of the analyzer was set at 40 eV for high-resolution spectra and 80 eV for survey scans, with energy resolutions of 0.05 and 1 eV, respectively. The spectra were analyzed using CasaXPS v.2.3.12Dev4 software. The C−C peak at 285 eV was used as the reference for binding energy calibration.

NEXAFS experiments were carried out on the U7A NIST/Dow materials characterization end-station at the National

Synchrotron Light Source at Brookhaven National Laboratory (BNL). The general underlying principles of NEXAFS and a description of the beamline at BNL have been previously reported.[58,59] The X-ray beam was elliptically polarized (polarization factor = 0.85), with the electric field vector dominantly in the plane of the storage ring. The photon flux was about 1×10^{11} photons per second at a typical storage ring current of 500 mA. A spherical grating monochromator was used to obtain monochromatic soft X-rays at an energy resolution of 0.2 eV. The C 1s NEXAFS spectra were acquired for incident photon energy in the range 270−320 eV. The angle of incidence of the X-ray beam, measured from the sample surface, was 50°. The partial-electron-yield (PEY) signal was collected using a channeltron electron multiplier with an adjustable entrance grid bias (EGB). Data were reported for a grid bias of −150 V. The channeltron PEY detector was positioned in the equatorial plane of the sample chamber and at an angle of 36° relative to the incoming X-ray beam. The PEY C 1s spectra were normalized by subtracting a linear pre-edge baseline and setting the edge jump to unity at 320 eV.[60] The photon energy was calibrated by adjusting the peak position of the lowest π^* phenyl resonance from polystyrene to 285.5 eV.[61]

Water contact angles were measured using a contact angle goniometer (AST Products, Inc. model VCA Optima XE) at room temperature. Dynamic water contact angle measurements were performed through the addition and retraction of a small drop of water (ca. 2 μL) on the surface. The advancing and receding contact angle behavior was digitally recorded and image analysis software was used to measure the angles.

Preparation of Surfaces for Algal Bioassays. Glass slides for bioassays were prepared as previously reported for SABCs based on the PS_{8K}-*b*-$P(E/B)_{25K}$-*b*-PI_{20K} precursor using Kraton G1652 SEBS as a thermoplastic elastomer base layer when forming the multilayer coating.[4] Glass slides coated with SABCs based on the PS_{8K}-*b*-$P(E/B)_{25K}$-*b*-PI_{10K} precursor subsequently were prepared in an analogous fashion using the new Kraton MD6945 SEBS in place of G1652. The rationale behind this change was that the elastic modulus of MD6945 (1.2 ± 0.3 MPa) is very similar to that of PDMS and lower than that of G1652 (18 ± 0.3 MPa).[57] The low modulus of PDMS is believed to contribute to its efficient fouling-release properties.[16,62−65] For all biofouling assays, glass microscope slides coated with a poly(dimethylsiloxane) (PDMS) elastomer, Silastic T2 (Dow Corning) prepared as described by Schumacher et al.[27] were included as standards and either slides coated with G1652 or MD6945 SEBS were included as controls. PDMS was used as a standard due to its excellent release properties against macrofouling organisms such as *Ulva* sporelings, while the G1652 or MD6945 base layers were used to highlight the differences in performance between the base layer alone and in the multilayer coatings.

Settlement of Zoospores and Strength of Attachment of Sporelings (Young Plants) of *Ulva*. Nine replicates of each test samples were leached in a 30 L tank of recirculating deionized water at ∼20 °C for 24 h before transferring to artificial seawater (ASW) 1 h prior to the start of the assays. Zoospores were released from fertile plants of *Ulva linza* and prepared for assay as described previously.[51] In brief, 10 mL of zoospore suspension (1×10^6 spores per mL), were pipetted into individual compartments of Quadriperm polystyrene culture dishes (Greiner Bio-One), each containing a test slide. The test slides were incubated in the dark at ∼20 °C for 1 h, then gently washed in seawater to remove zoospores that had not settled, i.e., were still motile. Three replicate slides of each type were fixed using 2.5% glutaraldehyde in seawater and were used to quantify the density of zoospores attached to the surfaces as previously reported.[66]

The remaining six replicates of each coating were used to culture sporelings (young plants).[67] A spore settlement assay was set up as described above, but after washing, the samples were transferred to dishes containing nutrient enriched seawater and grown for 7 days with the culture medium being refreshed every 48 h, under an 18 h−6 h light−dark regime at 18 °C. Growth was estimated by direct measurement of fluorescence, from chlorophyll contained within the chloroplasts of the sporelings, using a Tecan plate reader (GENios Plus).[68] Fluorescence was recorded as Relative Fluorescence Units (RFU), 300 readings per slide, taken in blocks of 30×10. The strength of attachment of the sporelings was determined by exposing the central area of biomass to an impact pressure delivered by a calibrated water jet.[69] The range of impact pressures used was chosen to provide maximum information about the strength of attachment of the sporelings. RFU readings (80 per slide) were taken from the central part of the slide that was exposed to the water jet. Percentage removal was calculated from the mean RFU reading before and after exposure to the water jet. From plots of percentage removal vs impact pressure, the critical water pressure required to remove 50% of the sporelings was derived. Slides coated with Silastic T2 supplied by Professor AB Brennan, University of Florida, were included as standards in the sporeling assays since PDMS is well-known for its fouling-release properties.[68]

Settlement and Strength of Attachment of *Navicula*. Cells of *Navicula* were cultured in F/2 medium contained in 250 mL conical flasks. After 3 days the cells were in log phase growth. Cells were washed 3 times in fresh medium before harvesting and diluted to give a suspension with a chlorophyll$_a$ content of approximately 0.25 μg mL^{-1}. The assay followed the same general principles as described for *Ulva*. Ten mL of cell suspension at ∼20 °C were added to each test surface. After 2 h, the slides were gently washed in ASW to remove cells that had not attached. Three of the six replicate slides were fixed, imaged and counted as described for zoospores of *Ulva*. Counts were made for 30 fields of view (each 0.064 mm^2) on each slide. The remaining three replicates were exposed to a shear stress of 20 Pa in a calibrated water channel.[70] The number of cells remaining attached was counted as described above.

Results and Discussion

Polymer Synthesis and Characterization. The synthesis of these two series of amphiphilic SABCs containing mixed discrete hydrophobic semifluorinated side-chains and hydrophilic PEGylated side chains was closely followed using both infrared spectroscopy and ^{1}H NMR. Following the epoxidation reaction, ^{1}H NMR studies clearly showed that there was no longer evidence of any alkene protons, and a significant peak at ca. 2.7 ppm

(58) Paik, M. Y.; Krishnan, S.; You, F.; Li, X.; Hexemer, A.; Ando, Y.; Kang, S. H.; Fischer, D. A.; Kramer, E. J.; Ober, C. K., Surface Organization, Light Driven Surface Changes and Stability of Semifluorinated Azobenze Polymers. *Langmuir* **2007**, *23*, 5110−5119.
(59) Genzer, J.; Sivaniah, E.; Kramer, E. J.; Wang, J.; Köerner, H.; Char, K.; Ober, C. K.; DeKoven, B. M.; Bubeck, R. A.; Fischer, D. A.; Sambasivan, S. *Langmuir* **2000**, *16*, 1993−1997.
(60) Samant, M. G.; Stöhr, J.; Brown, H. R.; Russell, T. P. *Macromolecules* **1996**, *29*, 8334−8342.
(61) Liu, Y.; Russell, T. P.; Samant, M. G.; Stöhr, J.; Brown, H. R.; Cossy-Favre, A.; Diaz, J. *Macromolecules* **1997**, *30*, 7768−7771.
(62) Berglin, M., Gatenholm, P. *J. Adhes. Sci. Technol.* **1999**, *13*, 713−727.
(63) Vladkova, T. *J. Univ. Chem. Technol. Metall.* **2007**, *42* (3), 239−256.
(64) Wynne, K. J.; Swain, G. W.; Fox, R. B.; Bullock, S.; Ulik, J. *Biofouling* **2000**, *16*, 277−288.
(65) Stein, J.; Truby, K.; Darkangelo-Wood, C.; Takemori, M.; Vallance, M.; Swain, G.; Kavanagh, C.; Kovach, B.; Schultz, M.; Wiebe, D.; Holm, E.; Montemarano, J.; Wendt, D.; Smith, C.; Meyer, A. *Biofouling* **2003**, *19*, 87−94.
(66) Callow, M. E.; Jennings, A. R.; Brennan, A. B.; Seegert, C. E.; Gibson, A.; Wilson, L.; Feinberg, A.; Baney, R.; Callow, J. A. *Biofouling* **2002**, *18*, 237−245.
(67) Chaudhury, M. K.; Finlay, J. A.; Chung, J. Y.; Callow, M. E.; Callow, J. A. *Biofouling* **2005**, *21*, 41−48.
(68) Finlay, J. A.; Fletcher, B. R.; Callow, M. E.; Callow, J. A. *Biofouling* **2008**, *24*, 219−225.
(69) Finlay, J. A.; Callow, M. E.; Schultz, M. P.; Swain, G. W.; Callow, J. A. *Biofouling* **2002**, *18*, 251−256.
(70) Schultz, M. P.; Finlay, J. A.; Callow, M. E.; Callow, J. A. *Biofouling* **2000**, *19* (supplement), 17−26.

Table 1. Percentage of Attachment of PEG550 and F10H10OH and Fluorine Content for Both Series of SABCs Produced from Different Molar Ratios of F10H10OH and PEG550 in the Reaction Feed

PS_{8K}-*b*-P(E/B)$_{25K}$-*b*-PI_{20K} Precursor						
feed % F10H10	feed % PEG550	attach % F10H10	attach % PEG550	overall attachment	wt % F	nomenclature
20	80	3	28	31	2.7	PS_{8K}-*b*-P(E/B)$_{25K}$-*b*-PI_{20}K-3F-28P
40	60	5	18	23	7.2	PS_{8K}-*b*-P(E/B)$_{25K}$-*b*-PI_{20}K-5F-18P
60	40	9	13	22	11.1	PS_{8K}-*b*-P(E/B)$_{25K}$-*b*-PI_{20}K-9F-13P
80	20	17	7	24	18.4	PS_{8K}-*b*-P(E/B)$_{25K}$-*b*-PI_{2}0K-17F-7P
PS_{8K}-*b*-P(E/B)$_{25K}$-*b*-PI_{10K} Precursor						
feed % F10H10	feed % PEG550	attach % F10H10	Attach % PEG550	overall attachment	wt % F	nomenclature
0	100	0	33	33	0	PS_{8K}-*b*-P(E/B)$_{25K}$-*b*-PI_{10}K-0F-33P
20	80	22	27	49	8.4	PS_{8K}-*b*-P(E/B)$_{25K}$-*b*-PI_{10}K-22F-27P
40	60	19	28	47	6.9	PS_{8K}-*b*-P(E/B)$_{25K}$-*b*-PI_{10}K-19F-28P
50	50	24	24	48	9.2	PS_{8K}-*b*-P(E/B)$_{25K}$-*b*-PI_{10}K-24F-24P
60	40	28	19	47	10.4	PS_{8K}-*b*-P(E/B)$_{25K}$-*b*-PI_{10}K-28F-19P
80	20	41	13	54	15.2	PS_{8}K-*b*-P(E/B)$_{25}$K-*b*-PI_{10}K-41F-13P
100	0	50	0	50	18.3	PS_{8K}-*b*-P(E/B)$_{25K}$-*b*-PI_{10}K-50F-0P

appeared indicating the presence of protons adjacent to the newly formed oxirane rings on the PI backbone. Additionally, infrared spectroscopy clearly showed the appearance of a C−O−C stretching peak at roughly 880 cm^{-1} associated with the epoxide ring. This indicated that all of the residual unsaturated alkene groups were successfully converted to their epoxidized form. The subsequent ring-opening reaction using F10H10OH and/or PEG550 alcohols led to the disappearance of the epoxide peak in the ^{1}H NMR spectra. Further analysis of the ^{1}H NMR spectra demonstrated the appearance of peaks at ca. 3.3 and 3.6 ppm for the PEG550 functionalized samples in combination with the appearance of a peak at ca. 3.5 ppm for the F10H10OH functionalized samples. This demonstrated successful attachment of the side groups. These findings were supported by infrared spectroscopy which demonstrated the appearance of a strong C−O stretching peak at 1120 cm^{-1} for samples functionalized with PEG550 and a strong C−F stretching peak at 1200 cm^{-1} for samples functionalized with F10H10OH. For mixed samples functionalized with both moieties, peak intensity generally varied with the relative amount of incorporation for each of the side chains.

Table 1 demonstrates the percentage of attachment of PEG550 and F10H10OH for each different molar feed ratio for both PS-*b*-P(E/B)-*b*-PI precursors. The percentage of PEG550 and F10H10OH successfully attached was calculated by ^{1}H NMR integration and elemental analysis of fluorine, respectively. Specifically, the percent attachment of PEG550 was obtained by comparing the total amount of aromatic protons (associated with the PS block) in the ^{1}H NMR spectra with the number of protons associated with the PEG side chain. Meanwhile, the weight percent of fluorine obtained by elemental analysis allowed the determination of F10H10OH attachment by comparing this value to that which would have been obtained assuming 100% attachment. The attachment of both PEG550 and F10H10OH depended on the molar ratios in the feed, and the overall attachment relative to epoxidized isoprene was between 22 to 30% for the PS_{8K}-*b*-P(E/B)$_{25K}$-*b*-PI_{20K} precursor and between 33 and 54% for the PS_{8K}-*b*-P(E/B)$_{25K}$-*b*-PI_{10K} precursor. Using GPC, the polydispersity of the samples was found to increase from 1.06 for both of the PS-*b*-P(E/B)-*b*-PI precursors to ca. 1.12 for their epoxidized forms. Finished, substituted SABC samples containing F10H10 and/or PEG550 side chains generally had a polydispersity between 1.2 and 1.3. This increase in dispersity combined with the observation of complete reaction of the epoxide despite less than 100% attachment suggested that some of the epoxide was lost due to intermolecular cross-linking reactions or the presence of trace water left in the reaction mixture.

It should be noted that these coatings do incorporate a potential perfluorooctanoic acid (PFOA) precursor moiety in the form of the F10H10 side group. Perfluorinated carbon chains eight carbons or longer (C8) have been discovered to bioaccumulate in mammals and are currently the attention of ongoing toxicological scrutiny.[71] While this decreases the likelihood of incorporating such a moiety in a commercial coating system, it does not take away from the fundamental information gained through the study. Additionally, current work is focused on extending these coating formulations to C6 (six perfluorinated carbon) and lower chain lengths, which are not known to have significant toxicological concerns and are anticipated to have greater processability.

Dynamic Water Contact Angles. For the samples derived from the PS_{8K}-*b*-P(E/B)$_{25K}$-*b*-PI_{20K} precursor polymer, advancing and receding water contact angles (Table 2) seemed largely dependent on the amount of hydrophobic F10H10 and hydrophilic PEG550 side chains that were incorporated in the SABC. As the amount of PEG550 incorporated in the coating increased in conjunction with a decrease in the amount of F10H10, water contact angles decreased from 128° to 103° (advancing) and from 67° to 28° (receding), suggesting that the presence of the surface active groups was greatly influencing wettability. The samples derived from the PS_{8K}-*b*-P(E/B)$_{25K}$-*b*-PI_{10K} precursor polymer did not show quite as clear a trend, however, with all the coatings except for PS_{8K}-*b*-P(E/B)$_{25K}$-*b*-PI_{10K}-0F-33P showing an advancing water contact angle ca. 125°. These high advancing contact values indicate that the surface has some level of roughness. Receding angles did show a slight trend, however, varying from 21° for PS_{8K}-*b*-P(E/B)$_{25K}$-*b*-PI_{10K}-0F-33P to 42° for PS_{8K}-*b*-P(E/B)$_{25K}$-*b*-PI_{10K}-50F-0P. High water contact angle hysteresis was demonstrated for both sets of SABCs, suggesting a dynamic surface capable of significant reorganization was realized in all cases. However, contact angle hysteresis was more pronounced for polymers derived from the PS_{8K}-*b*-P(E/B)$_{25K}$-*b*-PI_{10K} precursor. These observed differences in wettability behavior between each set of SABCs may be attributable to the combination of higher attachment and significantly higher side chain

(71) Lau, C.; Anitole, K.; Hodes, C.; Lai, D.; Pfahles-Hutchens, A.; Seed, J. *Toxicol. Sci.* **2007**, *99*, 366−394.

Table 2. Advancing and Receding Dynamic Water Contact Angle Measurements for Both Sets of SABCs Produced through the Incorporation of Different Amounts of the F10H10 and PEG550 Side Chains

PS_{8K}-*b*-$P(E/B)_{25K}$-*b*-PI_{20K} Precursor		
sample	$\Theta_{w,a}$	$\Theta_{w,r}$
PS_{8K}-*b*-$P(E/B)_{25K}$-*b*-PI_{20K}-3F-28P	103 ± 5	28 ± 3
PS_{8K}-*b*-$P(E/B)_{25K}$-*b*-PI_{20K}-5F-18P	118 ± 4	48 ± 3
PS_{8K}-*b*-$P(E/B)_{25K}$-*b*-PI_{20K}-9F-13P	124 ± 2	54 ± 2
PS_{8K}-*b*-$P(E/B)_{25K}$-*b*-PI_{20K}-17F-7P	128 ± 4	67 ± 4
PS_{8K}-*b*-$P(E/B)_{25K}$-*b*-PI_{10K} Precursor		
sample	$\Theta_{w,a}$	$\Theta_{w,r}$
PS_{8K}-*b*-$P(E/B)_{25K}$-*b*-PI_{10K}-0F-33P	104 ± 3	21 ± 4
PS_{8K}-*b*-$P(E/B)_{25K}$-*b*-PI_{10K}-22F-27P	125 ± 3	25 ± 3
PS_{8K}-*b*-$P(E/B)_{25K}$-*b*-PI_{10K}-19F-28P	128 ± 3	26 ± 4
PS_{8K}-*b*-$P(E/B)_{25K}$-*b*-PI_{10K}-24F-24P	128 ± 3	27 ± 4
PS_{8K}-*b*-$P(E/B)_{25K}$-*b*-PI_{10K}-28F-19P	127 ± 3	28 ± 3
PS_{8K}-*b*-$P(E/B)_{25K}$-*b*-PI_{10K}-41F-13P	127 ± 2	31 ± 2
PS_{8K}-*b*-$P(E/B)_{25K}$-*b*-PI_{10K}-50F-0P	126 ± 2	42 ± 4

grafting density realized for the PS_{8K}-*b*-$P(E/B)_{25K}$-*b*-PI_{10K} derived samples.

Despite the relatively low degree of polymerization of the surface-active segment (10K and 20K) in the unmodified polymers used for this study, it is not surprising that we observe similar surface behavior for both sets of materials and that the surface properties are dominated by the surface-active segment. As we modify the surface active block with PEG and fluorinated groups there is a substantial increase in the volume of each segmental repeat unit. For the polymer with the 10K segment, the modified block represents ~55% of the block copolymer volume assuming 50% attachment efficiency. Similarly, the polymer with the initial 20K segment, has after modification a block that represents ~70% by volume of the final polymer. Both of these materials as a consequence will likely tend to form structures with the resulting capacity to cover surfaces very well in the thin film structures we are testing. We have observed however that the polymers made with the longer PI 20K block appear less soluble likely as a result of the higher fluorine content in the polymer, thus making the shorter surface active segment more appealing for our purposes. Work is being conducted to better understand the microphase structure−property relationship of these materials.

X-ray Photoelectron Spectroscopy (XPS). Figure 1 shows high-resolution C 1s XPS spectra of amphiphilic SABCs derived from the PS_{8K}-*b*-$P(E/B)_{25K}$-*b*-PI_{10K} precursor with different extents of attachment of PEG550 and F10H10. The percentage attachment of F10H10 (F) and PEG550 (P) relative to epoxidized isoprene in the precursor is given in the figure legend. The spectra are normalized so that the total area under the carbon peaks is equal to unity. All polymers showed strong intensity peaks from C═C and C−C near 285 eV, indicative of the block copolymer backbone. There was clear evidence for all but the PS_{8K}-*b*-$P(E/B)_{25K}$-*b*-PI_{10K}-0F-33P sample of peaks associated with $-CF_2-$ and $-CF_3$ near 292 and 294 eV, respectively. As expected, the intensities of both $-CF_2-$ and $-CF_3$ decreased with increasing attachment of PEG550 and decreasing attachment of F10H10 in the mixture. A pronounced shoulder at ca. 287 eV associated with C−O was present in many of the samples, which can be attributed to both the ether-linked groups of the PEG550 moiety and also the alcohol functionality resulting on the polyisoprene block after ring-opening of the oxirane group.

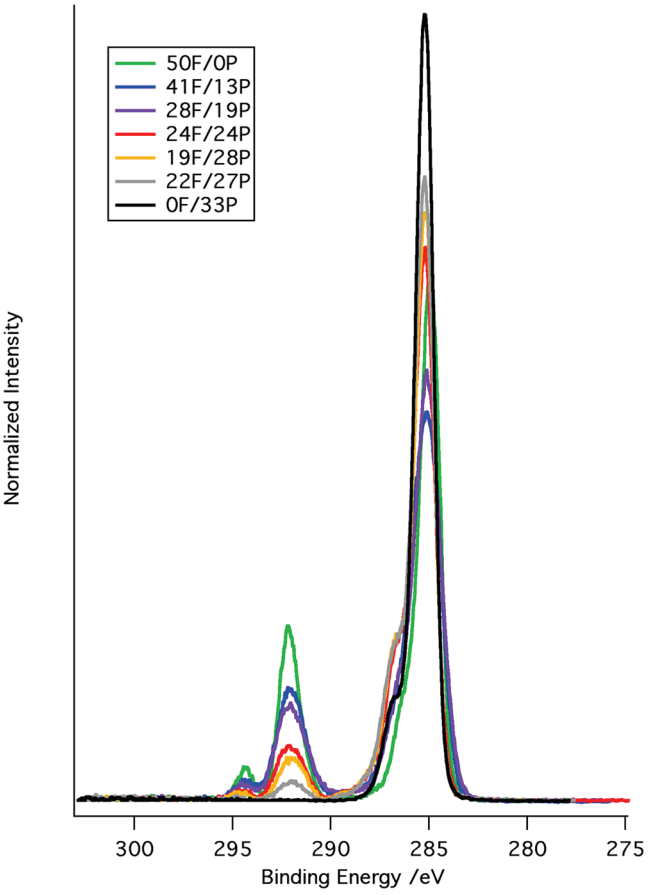

Figure 1. XPS C 1s spectra of the surfaces of amphiphilic SABCs containing mixed hydrophobic F10H10 and hydrophilic PEG550 side chains derived from the PS_{8K}-*b*-$P(E/B)_{25K}$-*b*-PI_{10K} precursor polymer taken at a 75° electron emission angle relative to the sample normal processed using Tougaard background subtraction. Sample labels give amounts of PEG550 (P) and F10H10 (F) side chains incorporated relative to epoxy functionality in the precursor polymer.

Near-Edge X-ray Adsorption Fine Structure (NEXAFS) Analysis. Figure 2 depicts the normalized C 1s NEXAFS spectra of spin-coated surfaces of amphiphilic SABCs derived from the PS_{8K}-*b*-$P(E/B)_{25K}$-*b*-PI_{10K} precursor with different amounts of PEG550 and F10H10 side chains attached taken at an angle of 50° between the surface and the soft X-ray beam. The characteristic C 1s → $\pi^*_{C=C}$ signals derived from the polystyrene block were observed near 285.5 eV for all seven of the spectra,[59] but the intensity of this peak was very low because the SABC surfaces were dominated by the PEG550 and F10H10 side chains. Other peak assignments can be based on calibrated NEXAFS spectra of poly(ethylene oxide) and poly(methyl methacrylate) as discussed in Krishnan et al.[49] The sharp resonance peak near 288 eV can be attributed to the C 1s → σ^*_{C-H} signal. This peak was particularly prevalent for the PS_{8K}-*b*-$P(E/B)_{25K}$-*b*-PI_{10K}-0F-33P sample, likely due to the absence of fluorinated moieties, indicating a surface dominated by the low surface energy poly(ethylene-*ran*-butylene) block, with possible contributions from the PEGylated moieties. The characteristic signals near 293 and 295.8 eV can be easily seen for the other six samples, and they are indicative of both the C 1s → σ^*_{C-F} and C 1s → σ^*_{C-C} resonances from the $-CF_2-$ helix, demonstrating the presence of the semifluorinated

(72) Genzer, J.; Kramer, E. J.; Fischer, D. A. *J. Appl. Phys.* **2002**, *92*, 7070−7079.

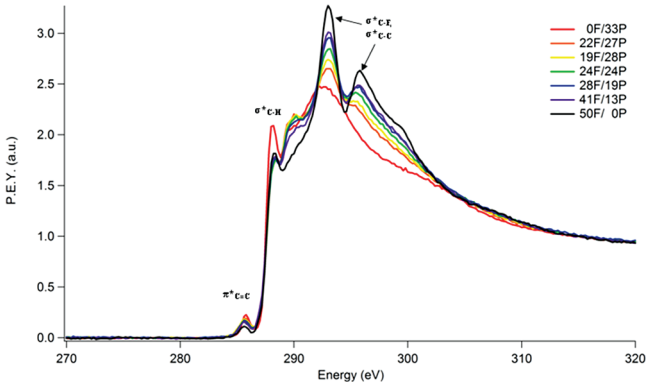

Figure 2. NEXAFS spectra of spin-coated surfaces of PS_{8K}-*b*-$P(E/B)_{25K}$-*b*-PI_{10K} derived SABCs on a silicon wafer after annealing at 120 °C for 12 h at an angle of 50° between the surface and the soft X-ray beam with major resonance transition peaks labeled.

groups on the surfaces.[72−75] The intensity profiles of the C 1s → σ^*_{C-F} signal were quite similar to those in XPS spectra which decreased with increasing incorporation of PEG550 and decreasing incorporation of F10H10OH in the mixture.

Settlement of Zoospores and Removal of Sporelings of *Ulva*. Figure 3A shows the settlement density of spores on G1652 SEBS and amphiphilic SABCs derived from the PS_{8K}-*b*-$P(E/B)_{25K}$-*b*-PI_{20K} precursor. The lowest settlement density was on the surface with 3% attachment of F10H10 and 28% attachment of PEG550. This result is generally consistent with behavior reported in the literature that indicates spores prefer to settle on a hydrophobic surface.[41] A green covering of sporelings was present on all test surfaces after 7 days of culture. The percentage removal of sporelings from the experimental coatings at a range of applied water jet pressures is shown in Figure 3B. Sporelings were removed from the PDMS standard at low water jet pressures reflecting the fouling−release characteristics of this low surface energy elastomer.[47,54] The applied water jet pressure required to remove sporelings from the amphiphilic SABCs surfaces derived from the PS_{8K}-*b*-$P(E/B)_{25K}$-*b*-PI_{20K} precursor largely depended on the relative incorporation of PEG550 and F10H10 side-chains. The surface with 3% attachment of F10H10 and 28% attachment of PEG550, which demonstrated the lowest spore settlement, required the highest applied water jet pressure of the four surfaces to effect the removal of sporelings. It was notable that the surfaces derived from the PS_{8K}-*b*-$P(E/B)_{25K}$-*b*-PI_{20K}-5F-18P and PS_{8K}-*b*-$P(E/B)_{25K}$-*b*-PI_{20K}-9F-13P SABCs required lower impact pressure than PDMS for effective sporeling release. This was especially true for the surface of PS_{8K}-*b*-$P(E/B)_{25K}$-*b*-PI_{20K}-5F-18P, for which ca. 95% sporelings were removed from the surface by an applied water jet pressure of only 24 kPa reflecting the excellent fouling-release properties of this polymer.

The set of SABCs derived from the PS_{8K}-*b*-$P(E/B)_{25K}$-*b*-PI_{10K} polymer were also evaluated for spore settlement and sporeling release to see if additional information regarding the fouling-release performance of these materials could be ascertained. Since this sample set was produced at a later date than that derived from the PS_{8K}-*b*-$P(E/B)_{25K}$-*b*-PI_{20K} polymer, it was hoped that the

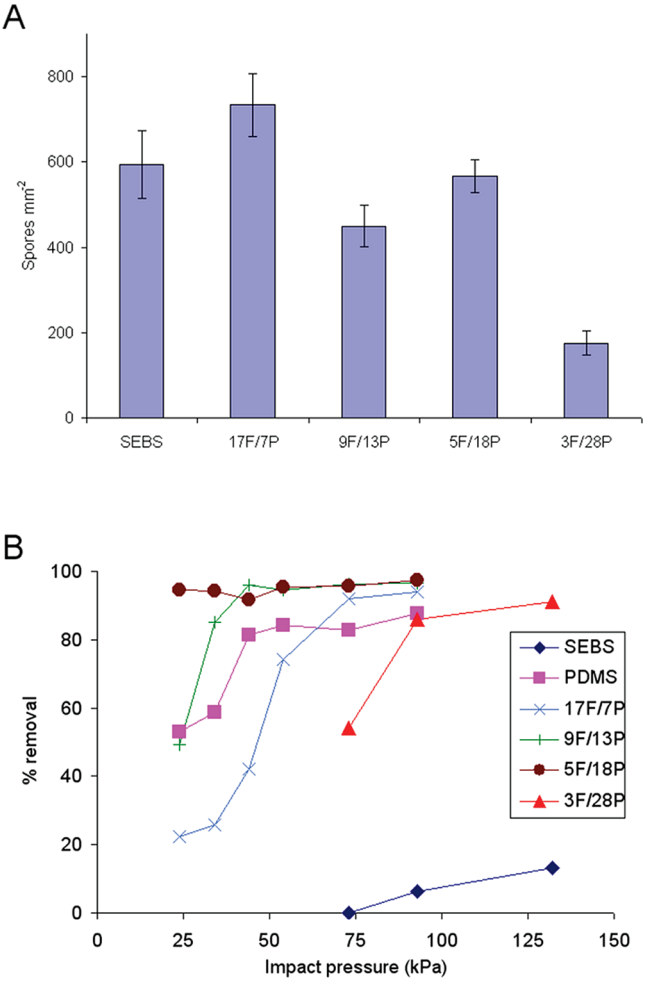

Figure 3. (A) The settlement of spores of *Ulva* on G1652 SEBS and PS_{8K}-*b*-$P(E/B)_{25K}$-*b*-PI_{20K} derived amphiphilic SABCs. Each point is the mean from 90 counts on 3 replicate slides. Bars show 95% confidence limits. (B) Percentage removal of 7-day old sporelings of *Ulva* from G1652 SEBS, PDMS (Silastic T2) and PS_{8K}-*b*-$P(E/B)_{25K}$-*b*-PI_{20K} derived amphiphilic SABCs. Slides were exposed to a water jet at a range of impact pressures; one slide was used for each pressure.

inclusion of purely PEGylated and purely fluorinated SABCs in conjunction with the more symmetric attachment distribution of side chains would aid in optimization of this approach.

Figure 4 shows the settlement density of spores of *Ulva* on MD6945 SEBS and SABCs derived from the PS_{8K}-*b*-$P(E/B)_{25K}$-*b*-PI_{10K} precursor. Trends were generally as expected and correlated very closely with the PS_{8K}-*b*-$P(E/B)_{25K}$-*b*-PI_{20K} derived samples, with those samples containing the largest proportion of the PEG550 side chain showing the lowest settlement. Figure 5 shows the results of the sporeling strength of attachment assay using a range of water jet pressures. While the lower boundary for relative incorporation of PEG550 to F10H10 side chains was not as well pronounced as was seen for the PS_{8K}-*b*-$P(E/B)_{25K}$-*b*-PI_{20K} derived coatings, both of the samples incorporating slightly more PEGylated than fluorinated side chains, along with the purely PEGylated sample, showed extremely promising fouling-release characteristics. When taken with the previous experiment, the sample incorporating 22% F10H10 and 27% PEG550 side chains appears to be particularly promising with regards to both anti-fouling i.e. inhibition of spore settlement and fouling−release. These results also suggest that a further iteration of testing focusing on samples incorporating slightly more of the PEGylated

(73) Genzer, J.; Sivaniah, E.; Kramer, E. J.; Wang, J.; Komer, H.; Xiang, M.; Char, K.; Ober, C. K.; DeKoven, B.; Bubeck, R. A.; Chaudhury, M. K.; Fischer, D. A. *Macromolecules* **2000**, *33*, 1882−1887.
(74) Genzer, J.; Sivaniah, E.; Kramer, E. J.; Wang, J.; Korner, H.; Char, K.; Ober, C. K.; DeKoven, B. M.; Bubeck, R. A.; Fischer, D. A.; Sambasivan, S. *Langmuir* **2000**, *16*, 1993−1997.
(75) Genzer, J.; Sivaniah, E.; Kramer, E. J.; Wang, J.; Xiang, M.; Char, K.; Ober, C. K.; Bubeck, R. A.; Fischer, D. A.; Graupe, M.; R. Colorado, J.; Shmakova, O. E.; Lee, T. R. *Macromolecules* **2000**, *33*, 6068−6077.

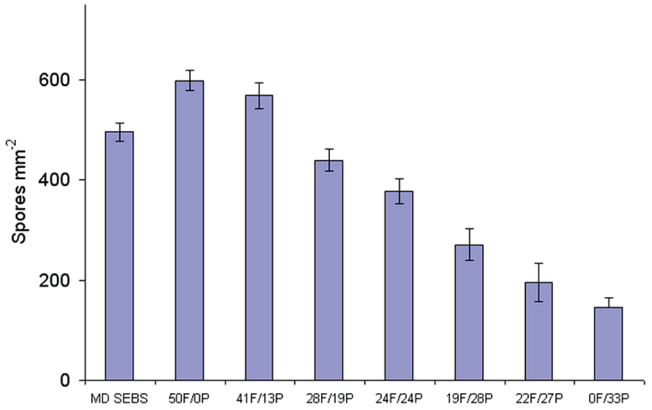

Figure 4. Settlement densities of spores of *Ulva* on PS_{8K}-*b*-$P(E/B)_{25K}$-*b*-PI_{10K} derived SABCs.

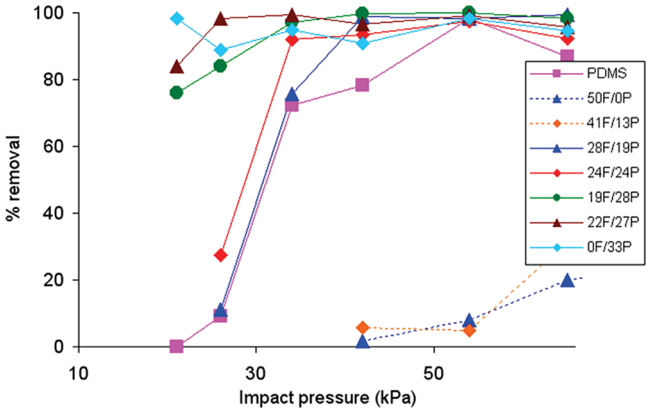

Figure 5. Percentage removal of sporeling biomass from PS_{8K}-*b*-$P(E/B)_{25K}$-*b*-PI_{10K} derived SABCs. Coated slides were exposed to the water jet over a range of water pressures; one slide was used at each pressure.

moiety than the fluorinated component could lead to further optimization of the system.

Table 3 summarizes the estimated critical pressure to release 50% of the attached sporelings of *Ulva* for both sets of coatings. The combination of the PS_{8K}-*b*-$P(E/B)_{25K}$-*b*-PI_{10K} derived SABCs with the MD6945 thermoplastic elastomer base layer led to a wide range of coatings that had fouling-release properties similar to, or better than, the PDMS standard.

Attachment of *Navicula*. Diatoms fall onto the surface of the samples by gravity, so that at the end of the 2 h settlement period, the same number of cells is in contact with all surfaces. Differences in the number attached cells after gentle washing and exposure to 20 Pa wall shear stress therefore reflect differences in their ability to adhere to the surface. Data are presented for SABCs derived from the PS_{8K}-*b*-$P(E/B)_{25K}$-*b*-PI_{10K} precursor, the MD6945 SEBS and PDMS (Silastic T2). Figure 6 shows there is a decrease in the number of cells attached as the content of PEG550 to F10H10 in the side chains increases. These data are consistent with the previous work that has shown that diatom cells attach less strongly to hydrophilic surfaces.[47,54,76] While the advancing contact angles for the SABCs derived from the PS_{8K}-*b*-$P(E/B)_{25K}$-*b*-PI_{10K} precursor show only relatively small differences with an increase in the content of PEG550 to F10H10 in the side chains, it would be expected that the differences in surface properties would

Table 3. Critical Surface Pressures for 50% Removal of Sporeling Biomass Derived from Removal Curves in Figures 3B and 5

PS_{8K}-*b*-$P(E/B)_{25K}$-*b*-PI_{20K} Precursor

sample	est. surface pressure for 50% removal (kPa)
PS_{8K}-*b*-$P(E/B)_{25K}$-*b*-PI_{20K}-3F-28P	70
PS_{8K}-*b*-$P(E/B)_{25K}$-*b*-PI_{20K}-5F-18P	< 25
PS_{8K}-*b*-$P(E/B)_{25K}$-*b*-PI_{20K}-9F-13P	25
PS_{8K}-*b*-$P(E/B)_{25K}$-*b*-PI_{20K}-17F-7P	45
PDMSe	25
G1652 M SEBS	> 250

PS_{8K}-*b*-$P(E/B)_{25K}$-*b*-PI_{10K} Precursor

sample	est. surface pressure for 50% removal (kPa)
PS_{8K}-*b*-$P(E/B)_{25K}$-*b*-PI_{10K}-0F-33P	< 21
PS_{8K}-*b*-$P(E/B)_{25K}$-*b*-PI_{10K}-22F-27P	< 21
PS_{8K}-*b*-$P(E/B)_{25K}$-*b*-PI_{10K}-19F-28P	< 21
PS_{8K}-*b*-$P(E/B)_{25K}$-*b*-PI_{10K}-24F-24P	29
PS_{8K}-*b*-$P(E/B)_{25K}$-*b*-PI_{10K}-28F-19P	31
PS_{8K}-*b*-$P(E/B)_{25K}$-*b*-PI_{10K}-41F-13P	165
PS_{8K}-*b*-$P(E/B)_{25K}$-*b*-PI_{10K}-50F-0P	250
PDMSe	31
MD 6945 SEBS	> 288

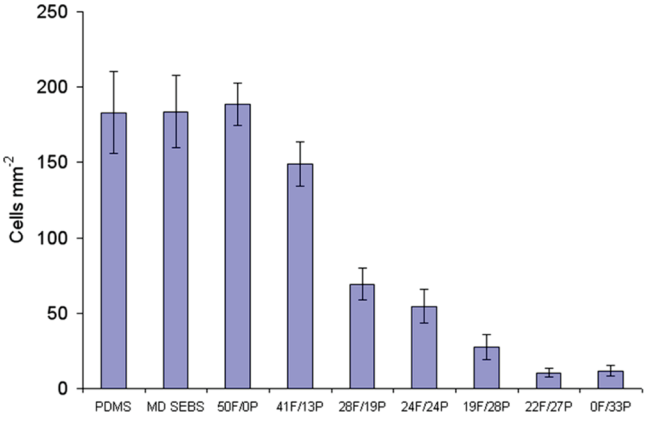

Figure 6. Number of diatom cells adhered to the surface of SABCs derived from the PS_{8K}-*b*-$P(E/B)_{25K}$-*b*-PI_{10K} precursor after gentle washing and exposure to 20 Pa wall shear stress in a flow channel. Means are derived from 90 counts, on each of three replicates. Bars show 95% confidence limits.

be greater for fully hydrated surfaces; it would be expected that the surface would restructure underwater leading to an increase in hydrophilicity and changes in surface nanotopography as shown for amphiphilic surfaces previously.[50] Recent data has indicated that diatom cells attached to hydrophilic surfaces are stressed, evidenced by elevated levels of nitric oxide, a signal molecule known to trigger stress responses in a wide range of organisms.[77] Diatom cells attached to hydrophobic PDMS have significantly lower amounts of nitric oxide and cells are attached more strongly to this surface.

Conclusions

Amphiphilic marine antifouling/fouling-release coatings were developed by chemical modification of two different polystyrene-*block*-poly(ethylene-*ran*-butylene)-*block*-polyisoprene ABC

(76) Holland, R.; Dugdale, T. M.; Wetherbee, R.; Brennan, A. B.; Finlay, J. A.; Callow, J. A.; Callow, M. E. *Biofouling* **2004**, *20*, 323−329.

(77) Thompson, S. E. M.; Taylor, A. R.; Brownlee, C.; Callow, M. E.; Callow, J. A. *J. Phycol.* **2008**, *44*, 967−976.

triblock copolymers with different combinations of hydrophilic PEG550 and hydrophobic F10H10 side chains. Resultant polymers were characterized using a combination of infrared spectroscopy, ^{1}H NMR spectroscopy, and elemental analysis, confirming that they contained a broad range of different relative amounts of PEG550 and F10H10. The surfaces of the polymers showed a high water contact angle hysteresis, suggesting a dynamic surface capable of significant reorganization. An increase in the incorporation of F10H10 side-chains to the polymer resulted in an increase in the intensity of the $-CF_2-$ and $-CF_3$ peaks for C 1s XPS analysis and 1s $\rightarrow \sigma^*_{C-F}$ resonance for C 1s NEXAFS measurements, suggesting segregation of this low surface energy moiety to the surface. The surfaces were evaluated with two common fouling algae, which have different modes of settlement and adhesion. In general, the lowest settlement of *Ulva* spores was seen on coatings containing a large proportion of PEG550 side-chains. The attachment strength of sporelings suggested that there is an optimal mixture of hydrophobic and hydrophilic side chains, biased toward a majority incorporation of PEG550. Of particular note was the potential to further optimize the coating system to obtain a fouling-release performance superior to that of PDMS, a known fouling-release material. The attachment of diatoms showed a more straightforward relationship, with fewer cells being attached to coatings that incorporated the highest amount of PEG550.

Acknowledgment. This work was supported by United States Department of Defense's Strategic Environmental Research and Development Program (SERDP), Grant WP #1454 with additional support from the Office of Naval Research (ONR) through Award Nos. N00014-08-1-0010 (J.A.C. and M.E.C.) and N00014-02-1-0170 (C.K.O. and E.J.K.). K.E.S. and E.J.K. acknowledge partial support from an NSF Graduate Fellowship and the NSF Polymers Program (DMR-0704539) as well as the use of facilities funded by the NSF-MRSEC program (UCSB MRL, DMR-0520415).

Supporting Information Available: A figure showing representative ^{1}H NMR spectra. This material is available free of charge via the Internet at http://pubs.acs.org.